

FORTY NEW INVARIANTS OF N -PERIODICS IN THE ELLIPTIC BILLIARD

DAN REZNIK, RONALDO GARCIA, AND JAIR KOILLER

ABSTRACT. We present some 40 newfound invariants displayed by N -periodics in the Elliptic Billiard, obtained through experimental exploration. These involve distances, areas, angles and centers of mass of N -periodics and associated polygons (inner, outer, pedal, antipedal). Some depend on the parity of N , others on other positional constraints. A few invariants have already been proven with elegant tools of Analytic and Algebraic Geometry. We welcome reader input to add to the list of proofs.

1. INTRODUCTION

The Elliptic Billiard (EB) is the only known integrable planar billiard [9]. Joachimsthal's Integral [15] implies that all trajectory segments are tangent to a confocal caustic, i.e., the EB is a special case of Poncelet's Porism [8], and therefore admits a 1d family of N -periodic trajectories. These imply a remarkable property: a family's perimeter is invariant [15, 13].

Here we catalogue some 40 newfound derived invariants observed via exploratory visualization and numeric measurement (non-combinatorial). These involve distances, areas, angles and centers of mass of N -periodics and associated polygons (inner, outer, pedal, antipedal, defined below). Indeed, some depend on the parity of N , others on other positional constraints.

While many invariants are readily observable, e.g., the sum of certain distances or the product/ratio of areas, the algebro-geometric techniques required to prove them are rather sophisticated and totally beyond our reach. Luckily, highly skilled and generous mathematicians have already contributed a few proofs [5, 6, 7].

The paper is organized as follows: preliminary definitions are given in Section 2. Invariants are tabulated in Section 3, in four parts: (i) Section 3.1 cover the earlier, basic invariants involving lengths, areas, and angles of N -periodics and associated polygons. (ii) Sections 3.2 and (ii) 3.5 describe invariants observed for pedal and antipedal polygons of N -periodics. Finally, in (iv) Section 3.6 invariants are described involving pairs of pedal polygons with respect to each focus.

Table 6 in Section 4 provides links to animations of the phenomena. All symbols used are compiled on Table 7 in Appendix A. Our experimental visualization tool is overviewed in Appendix B.

2. PRELIMINARIES

Let the EB have center O , semi-axes $a > b > 0$, and foci f_1, f_2 at $[\pm\sqrt{a^2 - b^2}, 0]$. Let a_c, b_c denote the major, minor semi-axes of the confocal caustic, whose values are given by a methdo due to Cayley [8], though we obtain them numerically.

Date: April, 2020.

Let $P_i, i = 1, \dots, N$ denote the vertices of an N -periodic trajectory. Let P'_i denote the vertices of the *outer polygon*, i.e., tangent to the EB at the P_i . Likewise, P''_i denotes the vertices of the *inner polygon*, marked by the points of tangency of the N -periodic to the caustic, Figure 1.

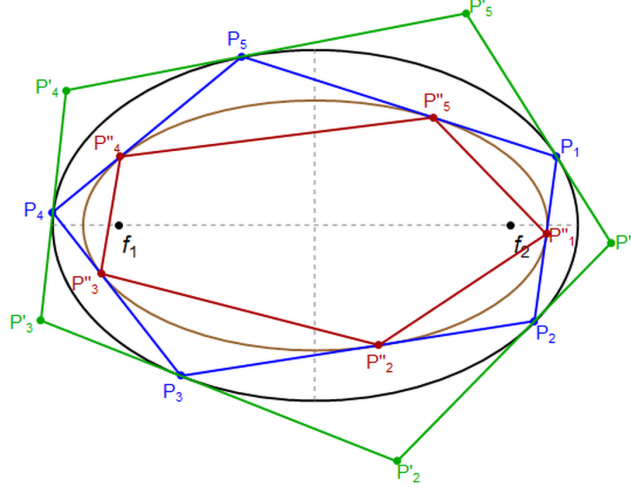


FIGURE 1. EB (black), with foci f_1, f_2 , a 5-periodic (blue) and the confocal caustic (brown). Also shown is outer polygon (green), tangent to the EB at the N -periodic vertices, and the inner polygon (red), whose vertices P''_i are defined by the points of tangency of the N -periodic to the Caustic.

As mentioned about, the perimeter L is invariant for a given N -periodic family, as is Joachmisthal's constant $J = \langle \mathcal{A}x, v \rangle$, where x is a bounce point (called P_i above), v is the unit velocity vector $(P_i - P_{i-1})/||\cdot||$, $\langle \cdot \rangle$ stands for dot product, and [15]:

$$\mathcal{A} = \text{diag} [1/a^2, 1/b^2]$$

Let a polygon have vertices $W_i, i = 1, \dots, N$. In this paper all polygon areas are *signed*, i.e., obtained from a sum of cross-products [10]:

$$(1) \quad S = \frac{1}{2} \sum_{i=1}^N W_i \times W_{i+1}$$

Let $W_i = (x_i, y_i)$, then $W_i \times W_{i+1} = (x_i y_{i+1} - x_{i+1} y_i)$.

3. INVARIANTS

In this section we present the invariants on four separate tables. Each is given an identifier k_{nmm} , where the first digit $n = 1, 2, 3, 4$ identifies whether the invariant is a basic, pedal, antipedal, or pairwise one.

3.1. Angles, Areas, and Distances. Invariants involving angles and areas of N -periodics and its tangential and internal polygons are shown on Table 1. There θ_i, A (resp. θ'_i, A') are angles, area of an N -periodic (resp. outer polygon to the N -periodic). A'' is the area of the internal polygon (where orbit touches caustic), see

code	invariant	value	which N	date	proven
k_{101}	$\sum \cos \theta_i$	$JL - N$	all	4/19	[5, 6]
k_{102}	$\prod \cos \theta'_i$?	all	5/19	[5, 6]
k_{103}	A'/A	?	odd	8/19	[5]
k_{104}	$\sum \cos(2\theta'_i)$?	all	1/20	[2]
k_{105}	$\prod \sin(\theta_i/2)$?	odd	1/20	[2]
k_{106}	$A'A$?	even	1/20	[7]
k_{107}	$k_{103}k_{105}$?	$\equiv 0 \pmod{4}$	1/20	?
k_{108}	k_{103}/k_{105}	?	$\equiv 2 \pmod{4}$	1/20	?
k_{109}	A/A''	k_{103}	odd	1/20	?
k_{110}	AA''	?	even	1/20	?
k_{111}	$A'A''$?	even	1/20	?
k_{112}	$A'A''/A^2$	1	odd	1/20	[3]
k_{113}	A'/A''	?	all	1/20	?
k_{114}	$\prod P_i - f_1 $?	$\equiv 2 \pmod{4}$	4/20	?
k_{115}	$\prod P'_i - f_1 $?	$\equiv 0 \pmod{4}$	4/20	?

TABLE 1. Distance, area, and angle invariants displayed by the N-periodic, its outer and/or inner polygon.

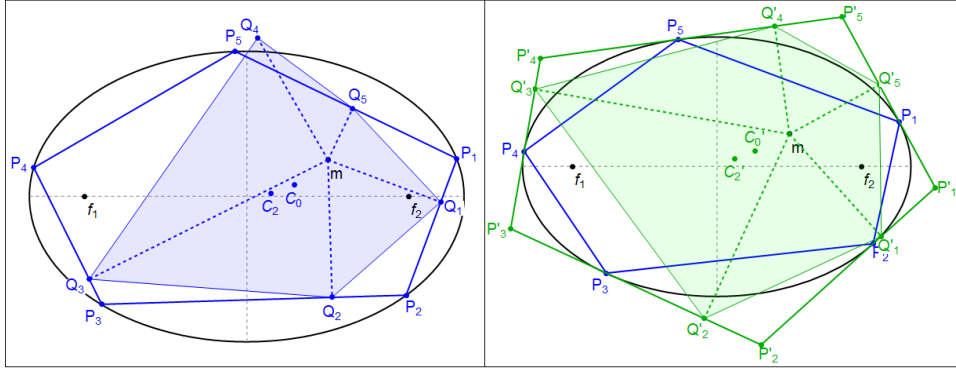


FIGURE 2. Left (resp. right): Pedal polygons for $N = 5$ from a point m with respect to the N -periodic (resp. its outer polygon). Vertex and area centroids C_0, C_2 are also shown.

Figure 1. All sums/products go from $i = 1$ to N . $k_{101}, k_{102}, k_{103}$ originally studied in [12].

3.2. Pedal Polygons. Tables 2 and 3 describe invariants found for the *pedal polygons* of N -periodics and the outer polygon, see Figure 2.

3.3. Pedals with respect to N-periodic. Let Q_i be the feet of perpendiculars dropped from a point M onto the sides of the N -periodic. Let A_m denote the area of the polygon formed by the Q_i , Figure 2. Let ϕ_i denote the angle between two consecutive perpendiculars $Q_i - M$ and $Q_{i+1} - M$. Table 2 lists invariants so far observed for these quantities.

code	invariant	value	which N	M	date	proven
k_{201}	$ Q_i - O $	a_c	all	f_1, f_2	4/20	[4]
$k_{202,a}$	$\prod Q_i - M $?	even	f_1, f_2	4/20	?
$k_{202,b}$	$\prod Q_i - M $?	$\equiv 0 \pmod{4}$	O	4/20	?
$k_{203,a}$	$A A_m$?	$\equiv 0 \pmod{4}$	all	4/20	?
$k_{203,b}$	$A A_m$?	$\not\equiv 2 \pmod{4}$	O	4/20	?
k_{204}	A/A_m	?	$\equiv 2 \pmod{4}$	all	4/20	?
k_{205}	$\sum \cos \phi_i$?	all	all	4/20	[1]

TABLE 2. Invariants of pedal polygon with respect to N-Periodic sides.

code	invariant	value	which N	M	date	proven
k_{301}	$ Q'_i - O $	a	all	f_1, f_2	4/20	[4]
k_{302}	$\sum Q'_i - M ^2$?	all	all	4/20	[6, Appendix]
$k_{303,a}$	$A' A'_m$?	$\equiv 2 \pmod{4}$	all	4/20	?
$k_{303,b}$	$A' A'_m$?	$\not\equiv 0 \pmod{4}$	O	4/20	?
k_{304}	A'/A'_m	?	$\equiv 0 \pmod{4}$	all	4/20	?
k_{305}	$\prod \cos \phi'_i$?	all	all	4/20	[1]
k_{306}	C'_0	?	all	all	4/20	[6, Appendix]
k_{307}	C'_2	?	even	all	4/20	?

TABLE 3. Invariants of pedal polygon with respect to the sides of the outer polygon.

3.4. Pedals with respect to the Outer Polygon. Let Q'_i be the feet of perpendiculars dropped from a point M onto the outer polygon. Let ϕ'_i denote the angle between two consecutive perpendiculars $Q'_i - M$ and $Q'_{i+1} - M$. Let A'_m denote the area of the polygon formed by the Q'_i .

In the spirit of [14] we also analyze centers of mass: $C'_0 = \sum_i Q'_i/N$ is the vertex centroid, and the *region* centroid C'_2 given by [10]:

$$\frac{1}{6S} \sum_{i=1}^N (W_i \times W_{i+1})(W_i + W_{i+1})$$

Where W_i, S , are a polygon's vertices and its signed area, (1). Table 3 lists invariants so far observed for these quantities.

3.5. Antipedal Polygons. The antipedal polygons to the N -periodic and the outer polygon are shown in Figure 3. The antipedal polygon Q_i^* of P_i with respect to M is defined by the intersections of rays shot from every P_i along $(P_i - M)^\perp$.

Let A_m denote the area of the Q_i^* polygon and C_0^*, C_2^* its vertex- and signed¹ area-centroids. $C_0'^*, C_2'^*$ refer to centers of antipedals of the outer polygon. Table 4 lists invariants found so far for these polygons.

¹Antipedals can be self-intersecting.

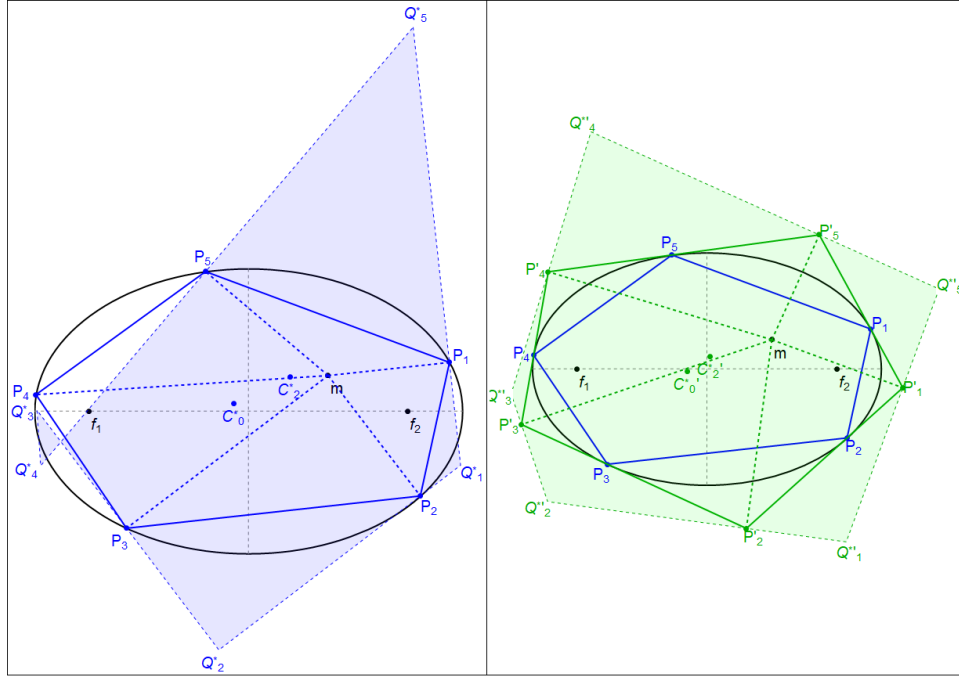


FIGURE 3. Left (resp. right): Antipedal polygons for $N = 5$ from a point m with respect to the N -periodic (resp. its outer polygon). Vertex and area centroids C_0^*, C_2^* are also shown.

code	invariant	value	which N	M	date	proven
k_{401}	$A' A_m^*$?	$\equiv 2 \pmod{4}$	all	4/20	?
k_{402}	A' / A_m^*	?	$\equiv 0 \pmod{4}$	all	4/20	?
$k_{403,a}$	$A_m A_m^*$?	odd	O	4/20	?
$k_{403,b}$	$A_m A_m^*$?	$\equiv 0 \pmod{4}$	f_1, f_2	4/20	?
k_{404}	A_m^* / A_m	?	$\equiv 2 \pmod{4}$	f_1, f_2	4/20	?
k_{405}	C_0^*	?	even	O, f_1, f_2	4/20	?
$k_{406,a}$	$C_0^{*'}, C_2^{*'}$	O	even	O	4/20	?
$k_{406,b}$	$C_0^{*'}, C_2^{*'}$?	4	f_1, f_2	4/20	?
k_{407}	$C_0^{*'}$?	even	f_1, f_2	4/20	?

TABLE 4. Invariants of antipedal polygons.

3.6. Pairs of Focal Pedals. Let $d_{1,i} = |Q_i - f_1|$, and $d_{2,i} = |Q_i - f_2|$. Let A_1 (resp. A_2) denote the area of the polygon formed by the feet of perpendiculars dropped from f_1 (resp. f_2) onto the N -periodic, and A'_1, A'_2 the same but with respect to the outer polygon. Table 5 list invariants so far detected involving pairs of these quantities.

Note $k_{602,a}, k_{602,b}$ can be proven via a symmetry argument, namely, area pair are equal since opposite vertices of an even N -periodic are reflections about the origin, as will be the pedal polygons from either focus.

code	invariant	value	which N	date	proven
k_{601}	$\sum d_{1,i} \sum d_{2,i}$?	odd	4/20	?
k_{602}	$\prod d_{1,i} \prod d_{2,i}$?	all	4/20	?
$k_{603,a}$	A_1/A_2	1	even	4/20	symm.
$k_{603,b}$	A'_1/A'_2	1	even	4/20	symm.
k_{604}	$A_1 A_2$?	odd	4/20	?
k_{605}	$A'_1 A'_2$?	odd	4/20	?
k_{605}	$A_1/A_2 = A'_1/A'_2$?	all	4/20	?

TABLE 5. Invariants between pairs of pedal polygons defined with respect to the foci.

4. CONCLUSION

Though not yet checked, we expect area ratio and product invariants similar to those listed on Table 5 to hold for pairs of antipedal polygons with respect to the foci, e.g., A_1^* , A_2^* and $A_1'^*$, $A_2'^*$.

To illustrate some of the above phenomena dynamically, we're prepared a [playlist](#) [11]. Table 6 contains links to all videos mentioned, with column "PL#" providing video number within the playlist.

PL#	Title	N	Narrated
01	Area Invariants of Pedal and Antipedal Polygons	3	yes
02	Exploring invariants of N-Periodics and pedal polygons	3–12	yes
03	Centroid Stationarity of Pedal Polygons	even N	yes
04	Concyclic feet of focal pedals and product of sums of lengths for odd N	5,6	
05	Invariant altitudes of N-Periodics and outer polygons I	3,4	
06	Invariant altitudes of N-Periodics and outer polygon II	5,6	
07	Sum of focal squared altitudes to outer polygon	3–8	
08	Sum of square altitudes from arbitrary point to outer polygon	5	
09	Area products of focal pedal polygons	5	
10	Area ratios of Pedal Polygons to N-Periodic and outer Polygon	5,6	

TABLE 6. Playlist of videos about invariants of N-Periodics. Column "PL#" indicates the entry within the playlist.

Given our focus on experimentation, we very much welcome reader contributions to add to the list of proofs.

REFERENCES

- [1] Akopyan, A.: Angles $\phi = \pi - \theta_i$ (resp. $\phi' = \phi - \theta'_i$), so equivalent to invariant sum (resp. product) of cosines. Private Communication (April, 2020) [4](#)
- [2] Akopyan, A.: Corollary of Theorem 6 in Akopyan et al., “Billiards in Ellipses Revisited” (2020). Private Communication (January, 2020) [3](#)
- [3] Akopyan, A.: Follows from previous results: the construction is affine and holds for any two concentric conics. Private Communication (January, 2020) [3](#)
- [4] Akopyan, A.: Perpendicular feet to N-periodic or its tangential polygon are cyclic. Private Communication (April, 2020) [4](#)
- [5] Akopyan, A., Schwartz, R., Tabachnikov, S.: Billiards in ellipses revisited (2020). URL <https://arxiv.org/abs/2001.02934> [1](#), [3](#)
- [6] Bialy, M., Tabachnikov, S.: Dan Reznik’s identities and more (2020). URL <https://arxiv.org/abs/2001.08469> [1](#), [3](#), [4](#)
- [7] Chavez-Caliz, A.: More about areas and centers of poncelet polygons (2020). URL <https://arxiv.org/abs/2004.05404> [1](#), [3](#)
- [8] Dragović, V., Radnović, M.: Poncelet Porisms and Beyond: Integrable Billiards, Hyperelliptic Jacobians and Pencils of Quadrics. Frontiers in Mathematics. Springer, Basel (2011). URL <https://books.google.com.br/books?id=QcOmDAEACAAJ> [1](#)
- [9] Kaloshin, V., Sorrentino, A.: On the integrability of Birkhoff billiards. Phil. Trans. R. Soc. A(376) (2018). DOI <https://doi.org/10.1098/rsta.2017.0419> [1](#)
- [10] Preparata, F., Shamos, M.: Computational Geometry - An Introduction, 2nd edn. Springer-Verlag (1988) [2](#), [4](#)
- [11] Reznik, D.: Playlist for “Invariants of N-Periodics in the Elliptic Billiard” (2020). URL <https://bit.ly/2xeVGYw> [6](#)
- [12] Reznik, D., Garcia, R., Koiller, J.: Can the elliptic billiard still surprise us? Mathematical Intelligencer (2019). DOI [10.1007/s00283-019-09951-2](https://doi.org/10.1007/s00283-019-09951-2). URL <https://arxiv.org/pdf/1911.01515.pdf> [3](#)
- [13] Rozikov, U.A.: An Introduction To Mathematical Billiards. World Scientific Publishing Company (2018) [1](#)
- [14] Schwartz, R., Tabachnikov, S.: Centers of mass of Poncelet polygons, 200 years after. Math. Intelligencer **38**(2), 29–34 (2016). DOI [10.1007/s00283-016-9622-9](https://doi.org/10.1007/s00283-016-9622-9). URL <http://www.math.psu.edu/tabachni/prints/Poncelet5.pdf> [4](#)
- [15] Tabachnikov, S.: Geometry and Billiards, *Student Mathematical Library*, vol. 30. American Mathematical Society, Providence, RI (2005). DOI [10.1090/stml/030](https://doi.org/10.1090/stml/030). URL <http://www.personal.psu.edu/sot2/books/billiardsgeometry.pdf>. Mathematics Advanced Study Semesters, University Park, PA [1](#), [2](#)
- [16] Wolfram, S.: Mathematica, version 10.0 (2019) [8](#)

APPENDIX A. TABLE OF SYMBOLS

symbol	meaning	note
O	center of billiard	
a, b	billiard major, minor semi-axes	
a_c, b_c	caustic major, minor semi-axes	
f_1, f_2	foci	
N	periodic vertices	
L	N -periodic perimeter	inv.
J	Joachimsthal's constant	inv.
P_i, P'_i, P''_i	N -periodic, outer, inner polygon vertices	
θ_i, θ'_i	N -periodic, outer polygon angles	
A, A', A''	N -periodic, outer, inner areas	
M	a point in the plane of the billiard	
Q_i, Q'_i	feet of perps. from point M to sides of N -periodic, outer polygon	
ϕ_i, ϕ'_i	angle between two consecutive perps. to N -periodic and outer polygon	
$Q_i^*, Q_i^{*'}$	vertices of the antipedal polygon from M with respect to the P_i, P'_i	
$d_{1,i}, d_{2,i}$	$ Q_i - f_1 , Q_i - f_2 $	
A_m, A'_m, A_m^*	area of Q_i, Q'_i, Q_i^* polygons	
A_j, A'_j	feet of perps. from $f_j, j = 1, 2$ onto the N -periodic, outer polygon	
C_0, C'_0, C_0^*	vertex centroids of the Q_i, Q'_i, Q_i^* polygons	
C_2, C'_2, C_2^*	area centroids of the Q_i, Q'_i, Q_i^* polygons	
$C_0^{*'}, C_2^{*'}$	vertex, area centroids of the $Q_i^{*'}$ polygon	

TABLE 7. Symbols used in the invariants.

APPENDIX B. EXPERIMENTAL LAB

Our main discovery tool was a custom-developed Wolfram Mathematica application [16] where N -periodics and their associated polygons could be computed, rotated, and analyzed, Figure 4. In particular, we could readily choose N , a particular configuration (parametrized by a location of a starting vertex on the EB), and the location of pedal points (see below). We could just as easily turn on and off the myriad of associated geometries.

As more evidence was gathered, new visualization and measurement functionality was added. The process of identifying whether a given quantity was invariant relied on first visual exploration and ideation, and then in writing code to display the measurement and its variance above the geometric picture.

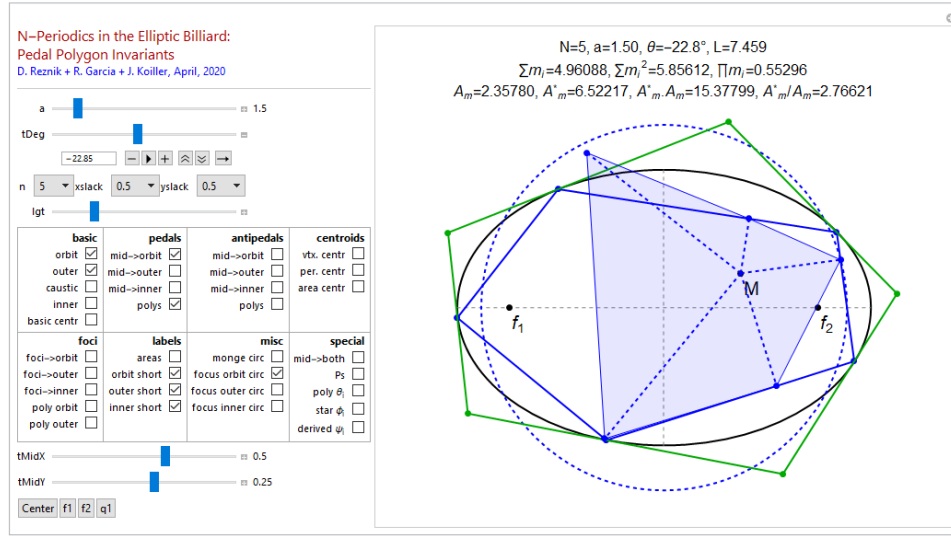


FIGURE 4. Our simulation tool.